

SIMULATION OF INUNDATION CAUSED BY TSUNAMI VIA UNDERGROUND CHANNELS

Kazunori ITO¹, Yukinobu ODA¹, Atsushi FURUTA¹ and Yuriko TAKAYAMA¹

Appropriate seawalls can protect landside from tsunami inundation. But, in a case that a coastal industrial facility has an underground water channel, even if a seawall works properly against tsunami attack, sea water comes into landside via the channel. So, this study focused on tsunami inundation via an underground channel caused by tsunami. Numerical simulation methods were discussed and verified by using physical model test results.

Keywords: tsunami; inundation; underground channel; overflow; two-phase simulation

INTRODUCTION

Tohoku Earthquake Tsunami, which has occurred on 11 March 2011, made us re-realize the importance and difficulty of protecting human life and infrastructures from devastating tsunamis (Mori and Takahashi 2012, Suppasuri et al. 2012). Hence, we have to re-consider whether we can expect all tsunami risk events without oversight from the view point of Business Continuity Plan (BCP). Usually, seawalls and dikes are constructed to stop the tsunami inundation. In case of industrial facilities facing to sea, such as a power plant, a chemical factory and so on, seawalls and dikes could protect the facilities from tsunami inundation. However, these facilities are often connected to the sea by the underground channels such as intake/outfall and drainage channels. Even if seawall functions properly against the tsunami inundation, sea water could come into the landward side via underground channels. This event is described as 'inundation inside seawall' (IIS). This research is focused on IIS, which was often overlooked as tsunami risk, and we studied about the simulation method of inundation on the landward side of the seawall comparing with a physical model test.

In hydraulic design phase of an underground intake/outfall channel and drainage channels connecting to the sea, surging analysis is executed normally in order to avoid overflow from pits. Surging phenomena in underground channels such as an intake/outfall and drainage channels is encouraged by high waves and tsunamis. In this process, water inside pits oscillates vertically during the time of high wave and tsunami attack. Since magnitude of the water oscillation is originated due to the resonant phenomena between configuration of the channels and wave period, a conventional one dimensional surging simulation is applied to confirm whether or not highest water levels in pits are below the ground level under the design conditions. If the conventional one dimensional simulation has an applicability to evaluate inundation on the landward side of the seawall caused by tsunami, it is very effective from an engineering view point.

So that, physical model tests were conducted to examine whether or not surging phenomena and inundation on the landward side of the seawall are similar (Fig. 1). And, two kinds of simulation methods were studied here. One of them is three dimensional simulation based on Volume of Fluid method (VOF). The other one is improved one dimensional surging simulation.

There is a possibility that inundation on the landward side of the seawall could occur due to storm surge. In a case of storm surge, lead time, that someone makes counter measures such as gate operation, plugging to avoid occurrence of inundation on the landward side of the seawall, is enough long. However, since earthquake and tsunami occur suddenly and people have to evacuate from tsunami, it is very difficult to make the counter measure actions in a case of tsunami. This is a different point about the inundation on the landward side of the seawall between a storm surge and tsunami.

HYDRAULIC PHYSICAL MODEL TESTS

Model Equipment and Experiment Cases

Hydraulic physical model test shown in Fig. 2 was conducted to investigate whether or not surging phenomena and inundation on the landward side of the seawall are similar phenomena. If distribution of overflow volume from pits corresponds to distribution of surging amplitudes in each pit, surging phenomena and inundation on the landward side of the seawall would be similar.

The physical model tests were carried out by using wave flume of Technology Center, Taisei Corporation. Slope type bathymetry was set in the flume. Long period regular wave was applied by

¹ Technology Center, Taisei Corporation, 344-1 Nase-cho Totsuka-ku, Yokohama, Kanagawa, 245-0051, Japan

non-reflected wave generator. Generated wave periods were 10s and 20s. The wave heights were 3cm, 5cm and 7cm. Underground pipe channels with 16mm and 31mm diameters were installed and five pits

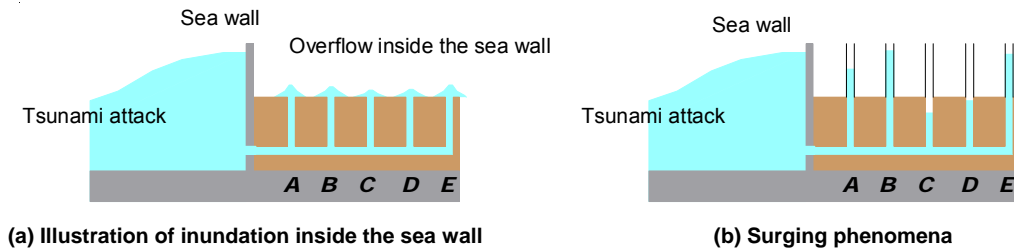


Figure 1. Explanation view of IIS and surging phenomena.

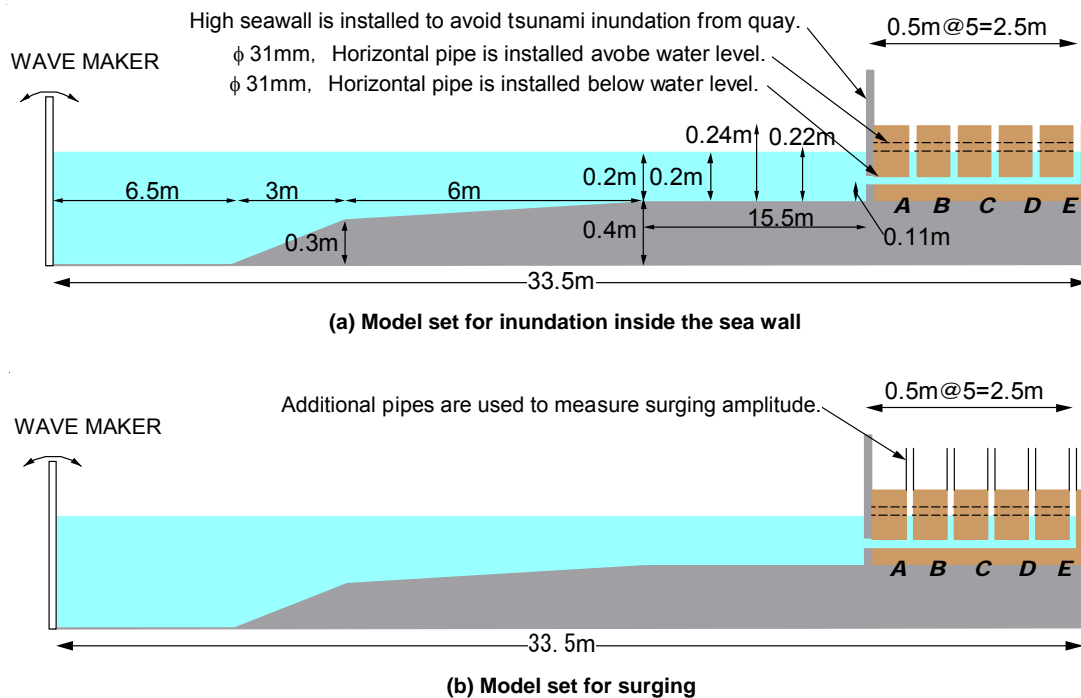


Figure 2. Schematic view of physical model test.

were also mounted. Interval between pits was kept as 0.5m constantly. Horizontal portion of the channels was set at two elevations. Difference of those was that horizontal portion was set under the water or in the air. Enough high sea wall was installed in order to stop land over flow from quay. Overflow water volume from pits was measured for different cases of IIS experiments shown in Fig. 2(a). Since generated wave period was long, the overflow volume was measured as sum up volume of first wave and second wave to minimize the influence of reflection wave from wave generator. Additional pits were mounted to measure the surging amplitude in the pits in case of surging experiments shown in Fig. 2(b). The surging amplitude was measured by using wave gauge in the case that pipe diameter was 31mm. But, since wave gauge was not able to be mounted inside $\phi 16\text{mm}$ diameter pit, the surging amplitude was not able to measure in the case of the $\phi 16\text{mm}$ diameter. The detailed description of the experiment conditions are presented in Table 1.

Results of Physical Model Test and Numerical Simulation

Objective of physical model test and numerical simulation is to evaluate whether or not surging is similar phenomena to inundation on the landward side of the seawall. So, difference between spatial

distribution of surging amplitude and spatial distribution of overflow volume from a pit is discussed as follows.

Fig. 3 shows tsunami wave profile in front of a quay and time series of surging at pit E. Location of pit E is shown in Fig. 2. Measurement results and numerical simulation results are indicated in Fig. 3. Two dimensional VOF method based on Navier-Stokes equations was applied for reproduction of tsunami wave profile. The simulation code is CADMAS-SURF (Isobe et al. 1999a, Isobe et al. 1999b, CDIT 2001). Conventional one dimension surging analysis was applied to reproduce time series of surging in pit E.

Experiment result of tsunami wave profile in Fig. 3 (a) has the soliton fission. Although there is discrepancy around crest portion of the wave profile with soliton fission, simulation results by using CADMAS-SURF reproduced experiment result qualitatively. It was a same situation about surging profile shown in Fig. 3 (b). Agreement between the experiment result and the conventional surging analysis results was substantially good. There is a clear difference between tsunami wave profile and surging profile. Tsunami profile has original 20s period oscillation mode and 1s period oscillation mode came from soliton fission. On the other hand, a surging profile shown in Fig. 3(b) has oscillation mode with about 5s. This 5s mode could be resonant mode of an underground pipe channel.

Table 1. Experiment conditions.				
Case	Horizontal pipe	Pipe and pits diameter [mm]	Wave height [cm]	Wave period [s]
AW-1	Under the water	31	7	20
AW-2	Under the water	31	5	20
AW-3	Under the water	31	7	10
AW-4	Under the water	31	3	10
AA-5	In the air	31	7	20
AA-6	In the air	31	7	10
AA-7	In the air	31	5	20
BW-1	Under the water	16	7	20
BW-2	Under the water	16	5	20
BW-3	Under the water	16	7	10
BW-4	Under the water	16	3	10
BA-5	In the air	16	7	20
BA-6	In the air	16	7	10
BA-7	In the air	16	5	20

Fig. 4 indicates distribution of maximum surging amplitude in a pit. Fig. 5 shows distribution of overflow water volume from a pit. In the case of maximum surging amplitude, the distribution was nearly flat or gradually increasing from A to E. But, in case of overflow water volume, the distribution was not flat and it was J shape. It means that overflow volume of pit A and E are larger among all pits while overflow volume of pit E is the largest. Distribution of overflow water volume is not similar to that of maximum surging amplitude.

If both distributions would be similar, we thought that surging analysis could be evaluation method to extract a large overflow volume pit before implementation of this experiment series. However, as shown in Fig. 4 and 5, since results of experiments was not similar between surging and overflow, it was found clearly that conventional surging analysis does not have applicability to estimate overflow water volume from pits. This is one conclusions of this experiment series (Ito et al. 2010).

A mechanism of difference between surging phenomena and overflow phenomena is discussed here. Backwater inside channel is governed by water difference of a pit back and forth. For instance, overflow volume from pit A increases in the occasion when water difference between pit B and tsunami height in front of a seawall is large. When overflow from each pit is continuing, the piezometric head of each pit is limited by ground elevation. It is inevitable that water difference of a pit

back and forth is very small. Dividing flow between a horizontal pipe and pit becomes weak and dominant momentum of backwater transports to terminal portion of channel. Since terminal portion is just bend shape, overflow from terminal pit increases. But, since tsunami surface elevation in front of a seawall is high, water difference between tsunami and pit B is always large. So, overflow from pit A is larger than pit B and C.

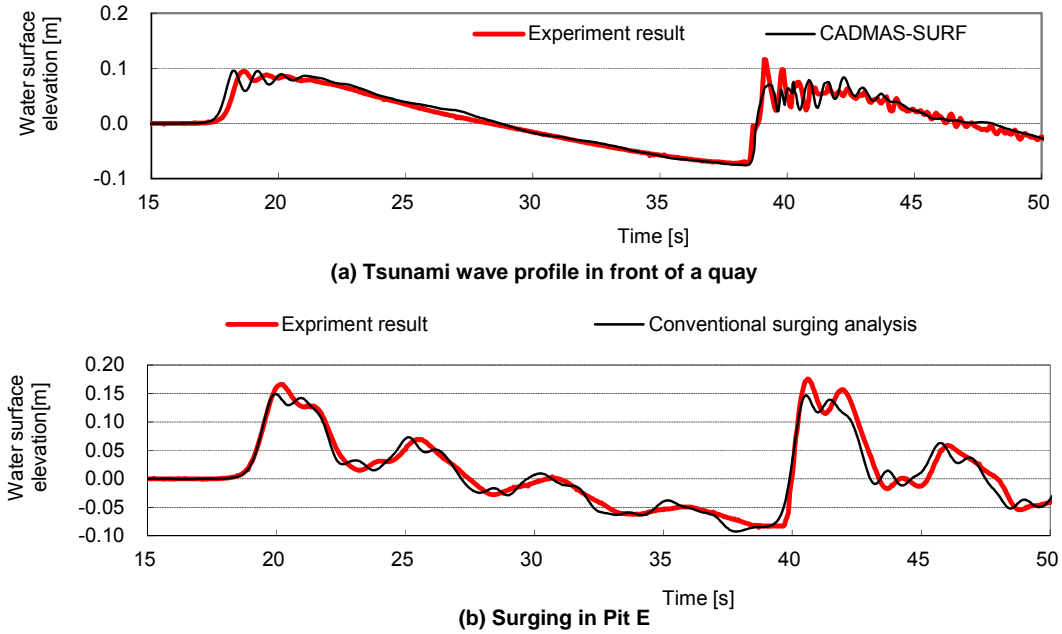


Figure 3. Time series of tsunami and surging profile. (Case AW-1)

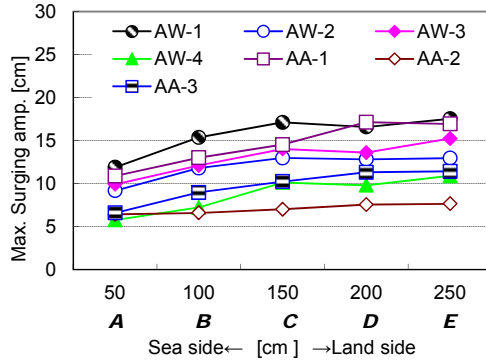
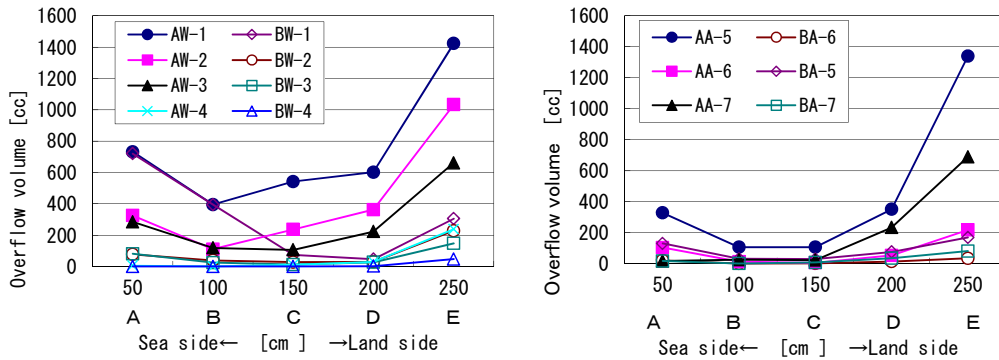


Figure 4. Distribution of maximum surging amplitude



(a) Horizontal pipe is set below SWL

(b) Horizontal pipe is set above SWL

Figure 5. Distribution of overflow water volume

THREE DIMENSIONAL NUMERICAL SIMULATION OF TSUNAMI OVERFLOW VIA UNDERGROUND CHANNELS

Simulation Method and Reproduce Simulation of Physical Model Test

As the simulation method, three dimensional two- phase (water and air) simulation model (CD-adapco 2010) was applied to reproduce the tsunami overflow volume. Governing equations are Navier-Stokes equations and Continuity equation. Simulation scheme is Finite Volume Method (FVM) and water surface was simulated using Volume of Fluid Method (VOF). Turbulence model, which had been used, is the standard k- ϵ model. Unstructured mesh system was employed as computational flexible mesh. Mesh size for both Δx and Δy varies from 0.004m to 1m. In case of Δz , mesh size varies from 0.004m to 0.01m.

Fig. 6 shows the comparison of overflow volume between physical model test and three dimensional numerical simulations. Simulation carried out for case AA-5 is shown in Fig. 6. Tsunami overflow volume given by the two- phase simulation has good accuracy. It was found high applicability of the two-phase simulation (Furuta et al. 2011).

Fig. 5 and Fig. 6 indicate very important matter from the view point of Business Continuity Plan (BCP). Overflow volume of terminal pit E, located landward side is largest. If an underground water channel shown in Fig. 2 is a water intake channel or a discharge channel of a power plant, normally a pump system is installed at pit E. Further, electric facility and devices are also set around pit E. Hence, there is high possibility of overflow attacks to the electric facilities and devices in this situation. In the case of a big tsunami attack to the industrial facility such as a power plant, an energy storage base and a chemical factory, a high seawall will be constructed in order to avoid land overflow from a quay. But, even if a high seawall worked properly, sea water comes into land side via an underground channel.

Physical model test shown in Fig. 2 does not have a special model scale. If the model scale is assumed as 1/100, diameter of the underground channel is nearly 3m and total length is 250m. Tsunami height is 7m. These size and condition are corresponding to a large-scale channel of power plant etc. So that, experiment results presented in this paper described that inundation inside seawall (IIS) is a risk event of tsunami BCP for industrial facilities located in seaside. Further, it emphasizes that IIS should not be ignored.

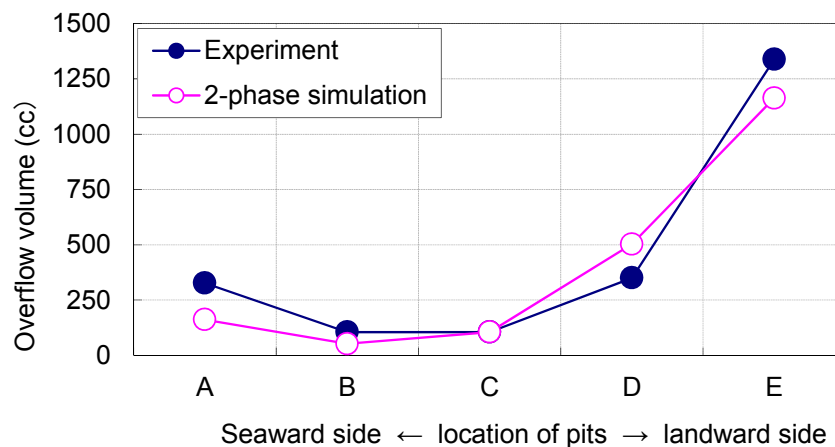


Figure 6. Comparison of overflow volume between experiment and numerical simulation

Case Study of Inundation Inside Seawall for Realistic Drainage Channel Network

An underground channel shown in Fig. 2 has simple shape and configuration. But, in the case of a real underground drainage channel for an industrial facility, the configuration is complex. Because diameter size of channel changes depending on location and some channels are connected at a point of a manhole. In this section, behavior of inundation on the landward side of the seawall in the case of a realistic underground drainage channel network is discussed.

Fig. 7(a) shows an image of a facility that has a realistic underground drainage channel network. It is assumed that the facility is some material storage base and plan scale is 300m x 300m. The facility has an enough high seawall that can stop tsunami overflow from a quay. There are roads in the model facility. A drainage channel network is buried under the roads. Parameters of the drainage channel network are plotted in Fig. 7(b). The drainage channel network consists of 4 lines (A, B, C, and D series). A1 to D2 are locations of each manhole. Parameters of the drainage channel network were designed based on Japanese water works design manual. Diameter of pipes varies from 0.3m to 1m. Diameter of manhole is 1m. Pipes are installed with slope. The slope is varies from 1/100 to 1/200. One drain point at quay is set to 1.8m below the still water level.

Fig. 8 shows computational mesh of a manhole potion. Computation was carried out according to the three dimensional two- phase (water and air) simulation model as described in previous section. Incident tsunami wave was long period regular wave with period 200s. Computational mesh size along the pipe axis direction varies from 0.12m to 3.08m. The mesh size along the right-angled direction to the pipe axis varies from 0.046m to 0.094m. The mesh size of vertical direction of manhole varies from 0.075m to 0.17m.

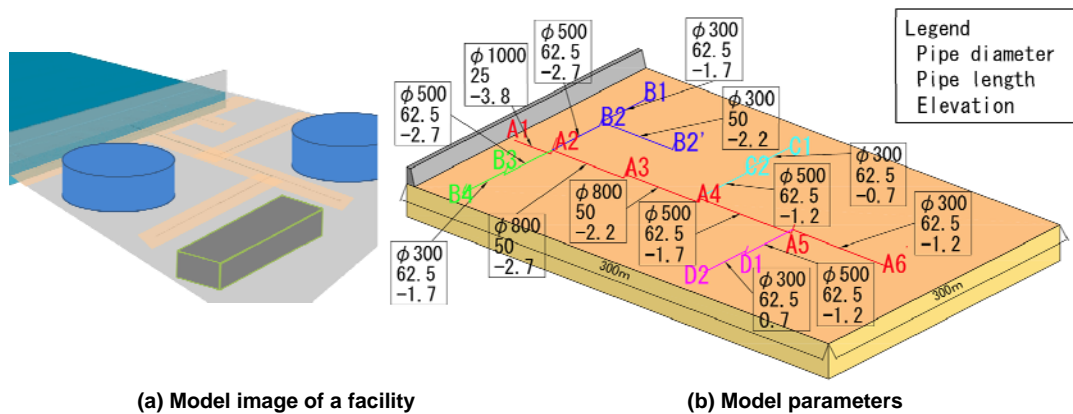


Figure 7. Model of a realistic underground drainage channel network

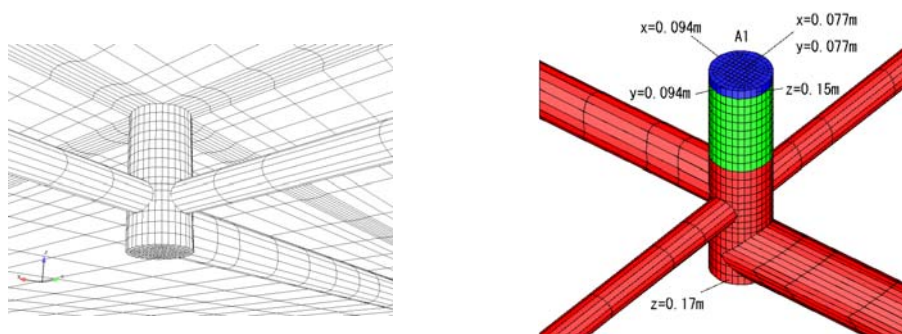


Figure 8. Computational mesh of a manhole portion.

Fig. 9 and Fig. 10 show the case study result for a realistic drainage channel network. Fig. 9 shows time series of water surface elevation in front of a seawall. As shown in Fig. 9, maximum water surface elevation is 9.4m. But, since height of a seawall is more than 9.4m, overflow from a seawall does not occur. In this case, overflow on the landward side of the seawall comes from each manhole. Fig. 10 shows snapshots of numerical simulation. These snapshots are situation of second tsunami attack. At first, overflow appeared at manhole A1, located just behind seawall. Overflow from other manholes also occurred and sea water comes from manhole A6 located at most landward side finally. Situation of first tsunami attack was similar to the situation of second attack. But, overflow from manhole A6 due to first tsunami attack is smaller than second wave attack.

Fig. 11 shows numerical simulation results under the ground. There is closed air in the pipe. When first tsunami attacked to a quay, an underground drainage channel was filled with sea water. And, overflow from a manhole started. In the occasion of backrush tsunami, seawater inside an

underground drainage channel started to return to the sea. Then free surface appeared in the pipes. Since discharge from the underground drainage channel took long time, second tsunami attack started before the completion of the discharge. Then, closed air was generated in the pipes. Since pipe system has slope as mentioned in previous section, seaside elevation of a pipe is lower than landside. If there is no flow velocity inside a pipe, closed air in a pipe could move toward the landside by the buoyancy and is exhausted via a manhole. However, closed air generated by second tsunami attack moved with sea water toward landside, it pushed sea water that remaining inside a pipe. So, the closed air encouraged overflow from landside manholes similar to the plug flow.

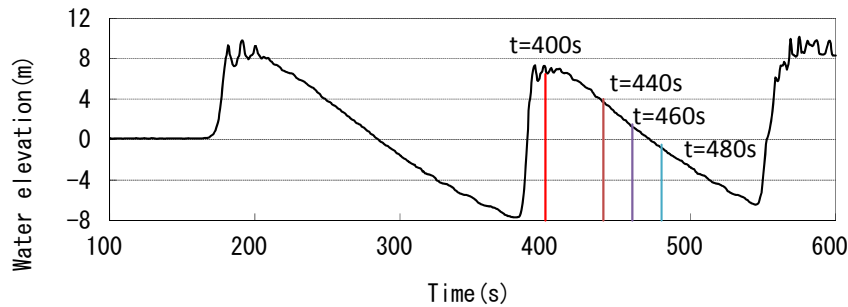


Figure 9. Time series of water surface elevation in front of a seawall

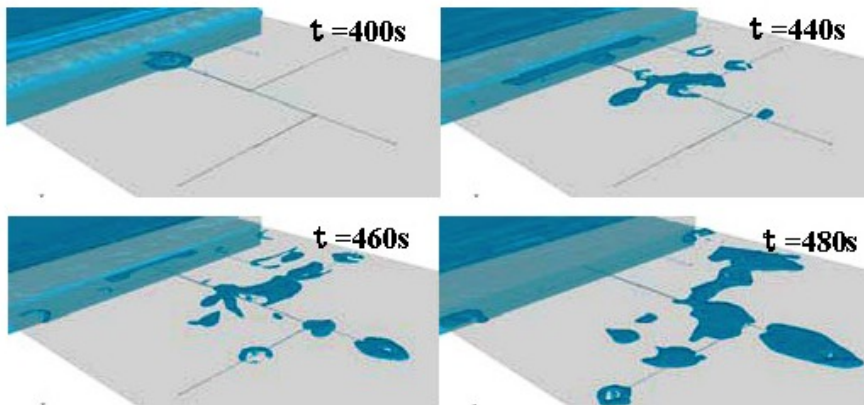
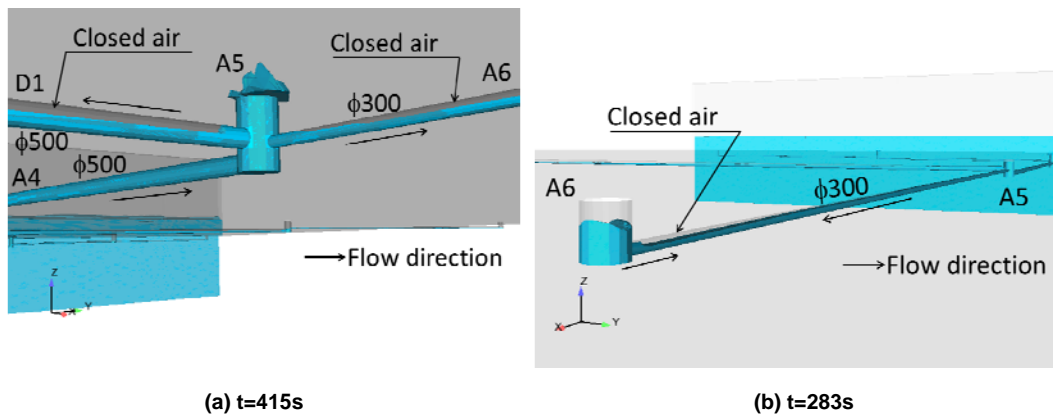


Figure 10. Snapshots of numerical simulation on the ground



(a) t=415s

(b) t=283s

Figure 11. Snapshots of numerical simulation under the ground

Fig. 12 shows overflow volume from each manhole. Since overflow volume of manhole A1 is much larger than the others, the result of manhole A1 is not included in Fig. 12. The volume in Fig. 12 is total volume due to first and second tsunami attack. There is a specific characteristic in overflow

volume distribution of A1 to A6 located in line. Overflow volume from seaward side manholes is large and the volume from landward side manholes is small. This trend is different from experimental results shown in Fig. 5. Since an underground drainage channel shown in Fig. 7 is more complex than the experiment model shown in Fig. 2, form loss of the underground drainage channel is also larger than the experiment model. It is a reason why there is the different trend. But, overflow volume from a terminal manhole A6 is larger than one of A5. It could be similarity between the underground drainage channel and the experiment model shown in Fig. 2. As the results, it was found that even if an underground drainage channel has complex configuration, inundation on the landward side of the a seawall could occur. Further, overflow from a terminal manhole located landward side occurs, even if the overflow volume is not so much.

This conclusion has an importance from a view point of BCP. This result describes that inundation inside a seawall (IIS) should be considered as one of the crucial tsunami risk events. Because, if the overflow reaches electric devices, the devices are definitely damaged. When the volume of the overflow is large, we could lose evacuation roots. Moreover, if evacuating people observe overflow in their ahead evacuation root, it could be hard to keep gentle refuge action.

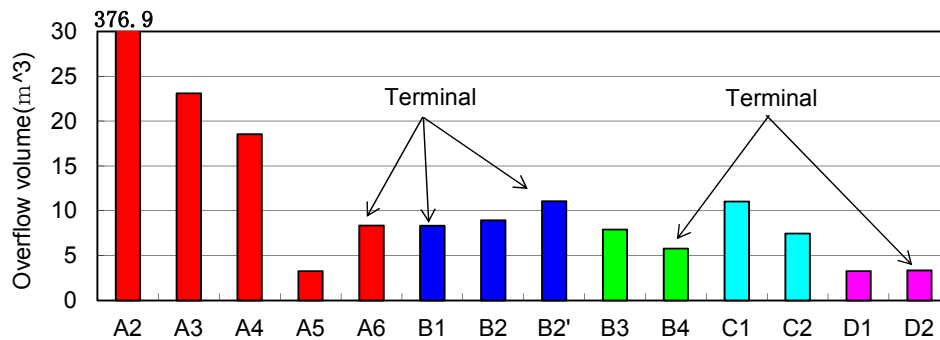


Figure 12. Snapshots of numerical simulation under the ground

STUDY OF ONE DIMENSIONAL SIMULATION MODEL

Applicability of three dimensional two-phase simulation for inundation inside seawall (IIS) was discussed in previous section. As an advantage of the simulation, output such as overflow volume, inundation area of overflow, the velocity and fluid force can be obtained. On the other hand, the simulation needs much effort to setup a model and takes long CPU time. These are disadvantages of the simulation. However, a simple simulation method, that is not much computationally expensive, is required from the view point of engineering. Even if an output from the simple simulation is only overflow volume, it could be enough as primary assessment of inundation on the landward side of the seawall. So that, one dimensional simulation model is studied here.

STUDY OF ONE-DIMENSIONAL SIMULATION MODEL

The three dimensional two-phase simulation for inundation inside seawall (IIS) was discussed in the previous section. That simulation can provide much information for inundation such as volume, inundation area, velocity and fluid force by the overflow water. However, that simulation requires much computational effort such as model setting and long CPU time. From an engineering standpoint, practical use gives an advantage on a simple simulation method. Then we developed a one-dimensional simulation model to estimate only the overflow volume, which gives primary assessment of inundation on the landward side of the seawall.

Formulation of One-Dimensional Simulation Model

Fig. 13 shows notations for the one-dimensional simulation model. For the sake of simplification, the cross-section areas of the main (horizontal) pipe and the vertical pit pipes are assumed to be constant as A_h and A_v respectively in this paper. In a common model for surging simulation, the pressure at the bottom of the pit (vertical pipe) is assumed to be equal to the water level of the pit, and

the acceleration of the water of the main pipe unit i is estimated as linear to the water level difference between the both end pipes ($\eta_i - \eta_{i-1}$). The difference equations derived from the continuity equation and the momentum equations for the common model are expressed as the following equations:

$$\frac{\Delta\eta_i}{\Delta t} = \frac{A_h(v_{i+1} - v_i)}{A_v} \quad (1)$$

$$\frac{\Delta v_i}{\Delta t} = \frac{g(\eta_i - \eta_{i-1})}{L_i} - [\text{loss}] \quad (2)$$

where the loss denotes the energy loss of head by the friction and the pipe form.

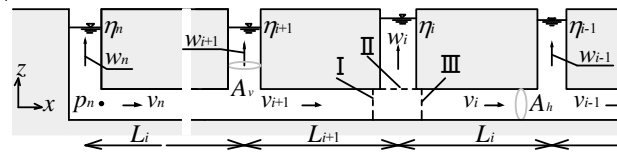


Figure 13. One-dimensional simulation model.

Fig. 14 shows the maximum surging amplitude and the overflow volume estimated by the above-mentioned common model compared with the model test results. As for the surging amplitude (Fig. 14(a)), the estimations show good agreement with the model tests. On the other hand, the estimated over flow volumes are much larger than the model test at the sea side pits, especially for large overflow cases. The local pressure differences in the vicinity of the bottom of pits (e.g., between I and III on Fig. 13) are neglected on the common model and it is considered to cause this error.

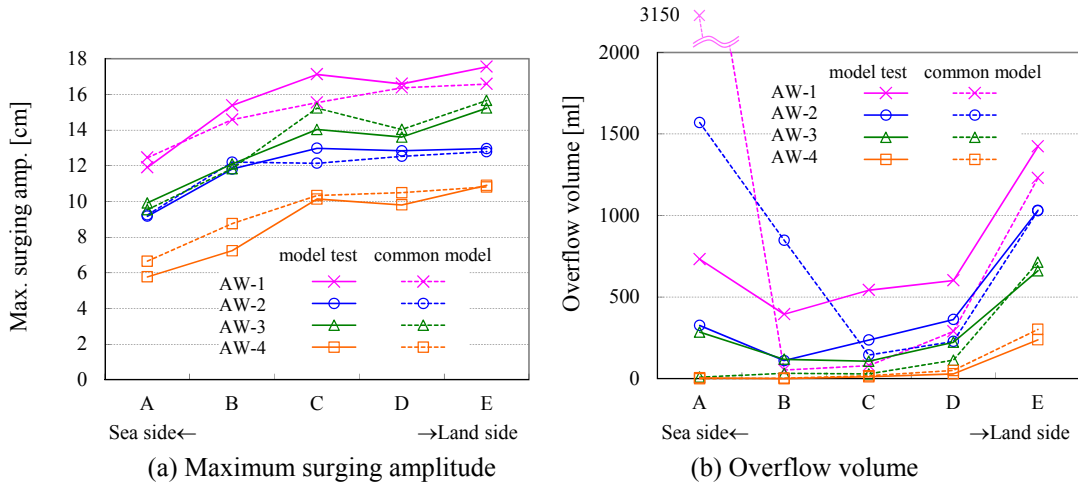


Figure 14. Comparison of the estimation by the common model with the model test.

As for the control area enclosed by the sections I, II and III in Fig. 13, the velocities at the sections are respectively represented as v_I , w_{II} and v_{III} . In the case of inflow ($v_{III} < 0$), the pit is also inflow ($w_{II} > 0$) and the bottom of pit is to be diversion. The absolute velocity of the section III is larger than that of the section I, so that the pressure at the section III should be less than that of the section I. On the common model, this pressure difference is neglected and it causes overestimations of the overflow of the sea side pit.

The energy loss coefficient for diversion is given as the following equation (Gardel 1957):

$$f_d = 0.58q_B^2 - 0.26q_B + 0.03 \quad (3)$$

where q_B is represented as the ratio of the flow rate of the branch pipe of the main pipe before diversion, i.e., $q_B = -w_{II} / v_I$ here. The pressure difference between the sections I and III are shown in Fig. 15 with the parameter of q_B . The broken line is derived from the difference of the velocity heads at the section I and III, which is calculated considering the energy loss by Eq. (3). The positive value means that the pressure at the section I is larger than that of the section III. The pressure difference

shown by the solid line in Fig. 15 is derived from only the difference of the velocity heads, not considering the local energy loss. When w_{II} is small, the energy loss is small and the pressure difference can be equal to the velocity head difference. When w_{II} becomes larger, the local energy loss cannot be neglected and the pressure difference becomes smaller than the velocity head difference. In this model, the pit velocities are assumed to be small compared with the main pipe velocity. The pressure difference generated at the vicinity of the pit bottom is assumed to be equal to the velocity head difference.

$$\Delta p_i = p_I - p_{III} = \rho(v_i^2 - v_{i+1}^2)/2 \quad (4)$$

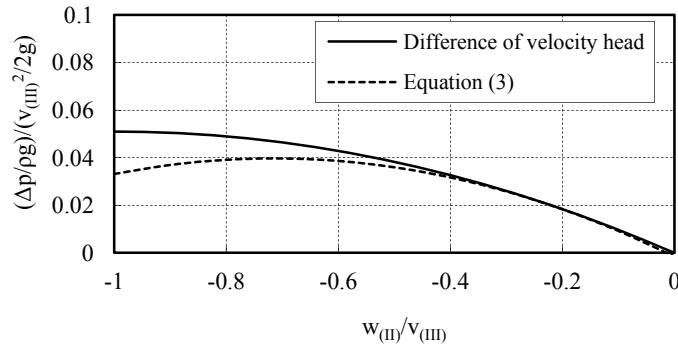


Figure 15. Difference of the pressure at diversion point.

In the case of confluence (e.g., $v_{III} < 0$, $w_{II} < 0$), the energy loss coefficient is given as the following equation (Gardel 1957):

$$f_c = -q_B^2(0.97 - 0.62\alpha) + q_B(1.94 - \alpha) + 0.03 \quad (5)$$

where q_B is represented as the ratio of the flow of branch pipe to the main pipe after confluence, and $q_B = -w_{II}/v_I$ here. α denotes the ratio of area A_v/A_h . Fig. 16 shows the pressure difference between the sections I and III derived with Eq. (5) in the same way of Fig. 15. In Fig. 16, the dot line shows the pressure difference calculated as the velocity head difference, and the solid line shows the pressure difference calculated as the momentum difference assuming that the momentum flux from the vertical pit is negligible. Opposite to the case of diversion, the pressure of the section I is less than that of the section III, because the velocity of the section I is larger.

Fig. 16 shows that when α is nearly equal to 0, the pressure difference calculated with Eq. (5) is equal to the momentum difference. Because the area of the pit A_h is much small and the velocity of the inflow from the pit is vertical like jet flow, there is no horizontal momentum flux from the pit. Therefore the pressure difference between the sections I and III occurs to balance the difference of the momentum. On the other hand, when $\alpha = 2.5$, the pressure difference may be approximated by the pressure difference calculated from the velocity head difference. When α is enough large, the vortex induced at the pit bottom is small, so that the energy loss is small. Hence the pressure difference equivalent for the difference of velocity head is occurred. Then the pressure difference is assumed to be linearly changing between the velocity head difference and the momentum difference according to α in this model, given as:

$$\Delta p_i = p_I - p_{III} = \rho(1 + \xi_i)(v_i^2 - v_{i+1}^2)/2 \quad (6)$$

where

$$\xi_i = \begin{cases} 0 & \text{for } \alpha > 2.5 \\ 1 - 0.4\alpha & \text{for } \alpha \leq 2.5 \end{cases}$$

The piezometric head of the main pipe at the upstream side for the pit (e.g., the section III for $v < 0$) is assumed to be equal to the total head. Then the pressure is represented with Eq. (7) and the momentum equation of the main pipe unit i is expressed as Eq. (8) when $v_i < 0$.

$$\begin{aligned}
 p_I &= \rho g \eta_i + \rho w_i^2 / 2 + \rho (1 + \xi_i) (v_i^2 - v_{i+1}^2) / 2 \\
 p_{III} &= \rho g \eta_i + \rho w_i^2 / 2 \quad \text{when } v_i < 0
 \end{aligned}
 \tag{7}$$

$$\frac{\Delta v_i}{\Delta t} = \frac{g(\eta_i - \eta_{i-1})}{L_i} + \frac{w_i^2 - w_{i-1}^2}{2} + \frac{(1 + \xi_{i-1})(v_i^2 - v_{i-1}^2)}{2L_i} - [\text{loss}] \quad \text{when } v_i < 0 \tag{8}$$

Comparing to Eq. (2), the second and the third terms of the right-hand are newly considered in this model.

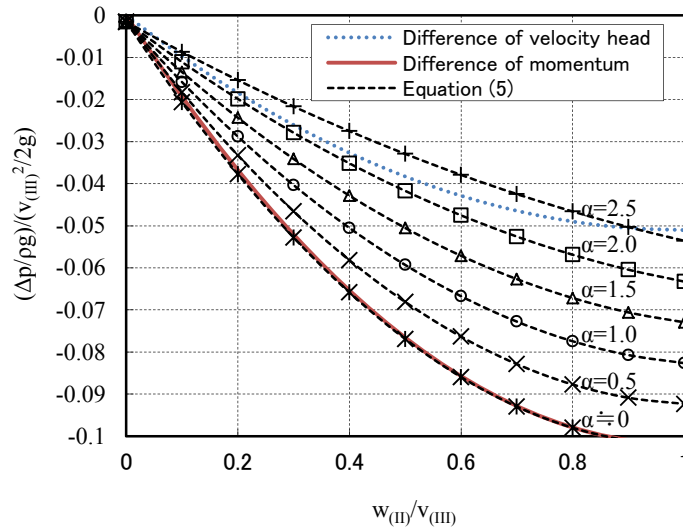
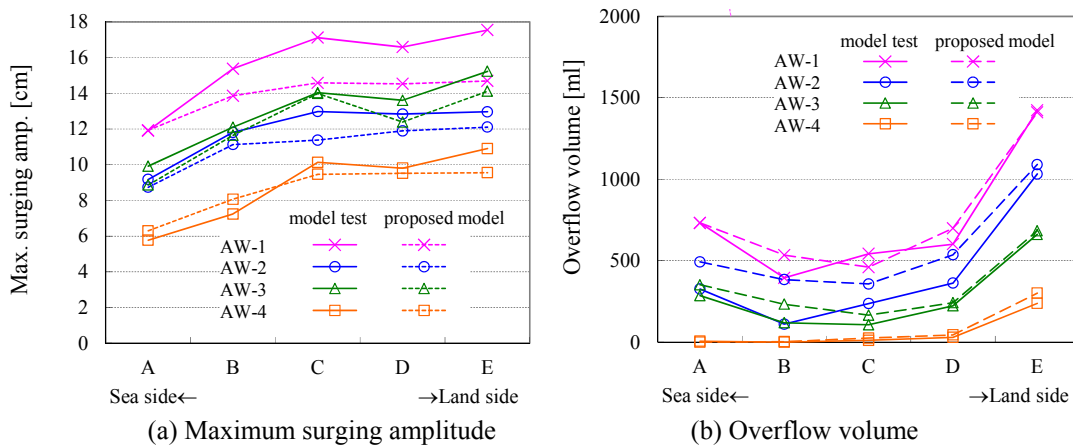


Figure 16. Difference of the pressure at confluence point.

Validation of One-Dimensional Simulation Model

Fig. 17 shows the comparison of the estimation by using Eq. (8) in the same way of Fig. 14. As for the surging (Fig.17 (a)), the proposed model reproduces the result of the model test with good accuracy similar to the common model (Fig. 14(a)). As for the overflow (Fig.17 (b)), the proposed model also has a good agreement with the model test result, comparing with the common model that cannot reproduce the model test shown in Fig. 14(b). It is found that it is necessary to consider the pressure difference at the bottom of the pit to estimate the overflow from the pit.

The validation comparing the calculation results by the proposed model and the common model with the model test result is shown in Fig. 18. The common model sometimes gives much overestimation, but the proposed model can reproduce the model test result with good accuracy.



(a) Maximum surging amplitude (b) Overflow volume
 Figure 17. Comparison of the estimation by the proposed model with the model test.

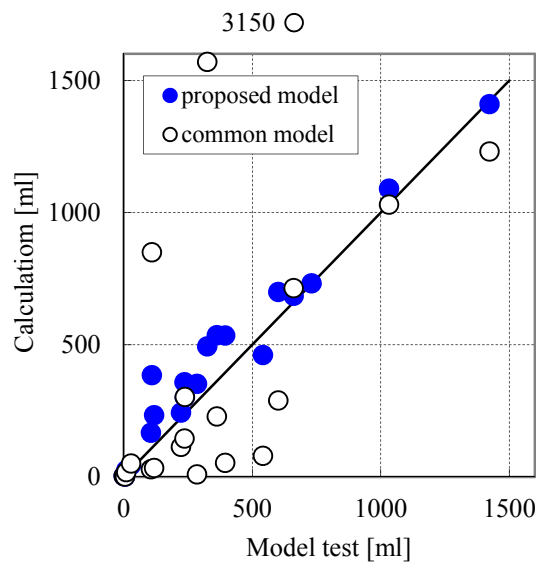


Figure 18. Comparison of the calculations with the model test.

CONCLUSION

This study is focused on tsunami inundation via an underground channel caused by tsunami. Appropriately installed seawall can protect landside from tsunami inundation. But, since coastal industrial facilities such as a power plant and a chemical factory and so on, use sea water, those are connected with underground water intake/water discharge channel. Even if a seawall functions properly against the tsunami attack, sea water could come into the landside via the channel. This phenomenon was called as inundation inside seawall (IIS) in this paper.

Characteristics of IIS were researched through hydraulic physical model test and three dimensional two-phase numerical simulation. In design phase of an underground channel, surging analysis is carried out in order to examine a relationship between the channel elevation and ground elevation. If the surging analysis has potential to evaluate IIS, it could be effective analysis. So that, surging phenomena and IIS were compared by using physical model tests. As the result, it was found that they have different characteristics. Especially, a remarkable characteristic of IIS was that overflow volume due to IIS was larger at landward side terminal pit. It was confirmed quantitatively using three dimensional two-phase numerical simulations, which could reproduce IIS phenomena including the remarkable characteristic. And it was pointed out that IIS should be considered as an important event from a view point of Business continuity plan for coastal industrial facilities. Additionally, it was demonstrated by using computational case study such that IIS could occur in case of a realistic underground drainage channel with complex shape and configuration, too. It was indicated that IIS is closely related to losing of evacuation routes during tsunami attack.

Although three dimensional two-phase numerical simulations has a high performance to evaluate IIS, the larger computational loads is one of the main disadvantage. Therefore, a simple simulation method, which is not computationally expensive, is required from a view point of engineering. Accordingly, one dimensional simulation method was developed and verified by using experiment results.

REFERENCES

- CD-adapco 2010, METHODOLOGY STAR-CD VERSION.4.14, CD-adapco.
- Coastal Development Institute of Technology of Japan, 2001. Research and development of a numerical wave flume; CADMAS-SURF, Report of the research group for development of numerical wave flume for the design of maritime structures, (in Japanese).
- Furuta, A., K. Ito and Y. Oda. 2011. Simulation of Overflow Phenomena via Underground Drainage Channels and Pits caused by Tsunami. Journal of JSCE, Ser. B2 (Coastal Engineering), Vol.67, pp.206-210. (in Japanese)

- Gardel, A., 1957, Les pertes de charge dans les écoulements au travers de branchments en te, Bulletin Technique de la Suisse Romande, No.9-10.
- Isobe, M., X. Yu, K. Umemura and S. Takahashi. 1999a. Study on Development of Numerical Wave Flume, *Proceedings of Coastal Engineering*, JSCE, Vol.46, pp.36-40. (in Japanese)
- Isobe, M.; Takahashi, S.; Yu, S.P.; Sakakiyama, T.; Fujima, K.; Kawasaki, K.; Jiang, Q.; Akiyama, M., and Oyama, H., 1999b. Interim development of a numerical wave flume for maritime structure design. *Proceeding of Civil Engineering in the Ocean 15*, JSCE, 321-326. (in Japanese)
- Ito, K., Y. Oda, Y. Takayama and A. Furuta. 2010. Basic Study on Overflow Phenomena via Underground Drainage Channels and Pits caused by Tsunami. *Journal of JSCE, Ser. B2 (Coastal Engineering)*, Vol.66, pp.941-945. (2010). (in Japanese)
- Mori, A., and T. Takahashi. 2012. Nationwide post event survey and analysis of the 2011 TOHOKU EARTHQUAKE TSUNAMI. *Coastal engineering journal, JSCE*, Vol.54, No.1, pp.125001-1-1250001-27.
- Suppasri, D., S. Koshimura, K. Imai, E. Mas, H. Gokon, A. Muhari and F. Imamura. 2012. Damage characteristic and field survey of the 2001 great east Japan tsunami in Miyagi prefecture. *Coastal engineering journal, JSCE*, Vol.54, No.1, pp.125005-1-1250001-30.